Journal of Solar Energy Research (JSER)

Journal homepage: www.jser.ut.ac.ir

The Airflow Energy Modelling In A Spiral Absorber In Static And Dynamic Situations

Sepehr Yousefbeigi[a], Hossein Ghadamian[a], Saeed Rahgozar[a], Elias Toozandeh Jani[a]

[a] *Department of Energy, Materials and Energy Research Center, Karaj, Iran.*

ARTICLE INFO

Article Type:

Research Article

Received:25.11.2023
Accepted:12.10.2024

Keywords:
MATLAB open source code software
Static and dynamic modeling
spiral absorber
cell temperature
heat dissipation

A B S T R A C T

The absorption of sunlight causes solar panels to heat up, and the resulting temperature plays a crucial role in determining the amount of output voltage. In this study, a novel spiral geometry was developed behind the Tedlar layer of photovoltaic panels (PVs) to regulate the dissipation of heat by air. Dynamic and static numerical modelling was conducted using open-source MATLAB software. The first step involved determining and simultaneously solving mathematical equations to obtain the desired geometry. A comparison of static modelling revealed that in identical environmental conditions, the electrical efficiency of the system (temperature of the cell) was approximately 7.5% and 10% (58 ºC and 53 ºC), without and with the use of a heat absorber, respectively. In the subsequent phase, a variable speed fan with a maximum power of 2 watts was employed behind the panel to cool the system. Dynamic modelling showed that the system efficiency and cell temperature were 7.4% and 58.5 ºC, respectively. By using a spiral thermal absorber, under similar environmental conditions, the cell temperature decreased to 54 ºC, and the system efficiency was improved to 9.2%. According to dynamic modelling, a reduction of 8% in panel temperature could be achieved.

1. Introduction

Photovoltaic panels (PVs) convert sunlight directly into electricity. However, their efficiency decreases as the ambient temperature increases. This version emphasises the effect of temperature on efficiency rather than the amount of electricity directly [1]. To mitigate this issue, researchers have proposed different methods for cooling PV systems. Among them, using air as a working medium is the most available and least expensive approach [2]. Researchers in the field of improving the thermal and electrical efficiency of PV systems have reviewed various approaches and provided solutions. Current research investigates modifying the geometry of PV systems to achieve improvements in both electrical and thermal efficiency. Forced convection can achieve higher thermal efficiency by changing variables such as airspeed and increasing the flow rate, although it presents a challenge in the energy balance of the system. Researchers hope to boost thermal efficiency by using fans and embedding

*Corresponding Author's Email: h.ghadamian@merc.ac.ir

Cite this article: Yousefbeigi, S., Ghadamian, H., Rahgozar, S., & Toozandeh, E. (2024). The Airflow Energy Modelling In A Spiral Absorber In Static And Dynamic Situations. Journal of Solar Energy Research, 9(3), 1994-2009. doi: 10.22059/jser.2024.367968.1356

DOI: 10.22059/jser.2024.367968.1356

channels under Tedlar. Cuce et al. [3] cooled PV panels using rectangular fins and air and achieved a thermal efficiency of approximately 30% with a heat flux density of 600 W/m^2. Brinkworth and Sandberg [4] found that the length-to-hydraulic diameter ratio of a rectangular channel significantly impacts thermal efficiency. Their study showed that a ratio of 20 resulted in a 38% increase in thermal efficiency. In a study conducted by Hernandez et al. [5] the impact of active cooling on the output power of PVs was investigated. The researchers designed and tested three types of channels with different dimensions and found that an increase in airspeed led to a rise in output power. Their results also showed that PVs generated more electrical power with a fan than with passive cooling at the same radiation intensity and channel dimensions. Özakin et al. [6] used Ansys Fluent software to simulate the effects of cylindrical cylinders in cooling photovoltaic panels and observed a decrease in panel surface temperature of 10-15°C due to slower airflow near the cylinders from friction and viscous forces. Temperature contour images from the software were consistent with experimental values. Positioning the cylinder beneath the solar panel resulted in less thermal stress on the panel. Sopian et al. [7] investigated the thermal efficiency of a two-pass flat-plate solar collector that employed either a single-pass channel or two reciprocating channels. The researchers determined that the maximum thermal efficiency achieved with the single pass channel and the two reciprocating channels were approximately 32.5% and 42.5%, respectively. They concluded that the use of two reciprocating channels resulted in significantly higher thermal efficiency than the single pass channel and that the system was economically significant due to the use of relatively low-cost materials and components Almuwailhi and Zeitoun [8] conducted a study on natural convection, forced convection, and evaporation cooling techniques for PVs in Saudi Arabia. Their experiments showed that the use of evaporation cooling increased electricity efficiency by 3.8%. They also found that natural convection increased electrical efficiency by 1.7%, while forced convection increased it by 4.4%. Vajedi et al. [9] experimented in Karaj, Iran, to compare the thermal efficiency of convergent and normal channels for cooling photovoltaic panels. Sadaq et al. [10], found that the thermal efficiency in the convergent channel was 5% higher with two fans and 15% higher with four fans, compared to the normal channel. They also presented an experimental correlation based on thermodynamic relations between the panel temperature and the convective heat transfer coefficient Improving the thermal efficiency of a photovoltaic panel generally leads to better performance. Proper airflow geometry can achieve up to 50% thermal efficiency, and forced convection can triple the thermal efficiency compared to natural convection. Technological advancements have greatly improved the electrical efficiency of PVs, with modern panels reaching up to 20% efficiency. Researchers have suggested using cooling fluids or controllers to further increase electrical efficiency and maximise the output of the panel. Othman et al. [11] designed triangular channels made of aluminum to enhance the electrical efficiency of a photovoltaic thermal (PVT) double-pass air collector. Their experiments demonstrated that this design increased the electrical efficiency by approximately 1%. These research findings provide valuable insights into the design and optimisation of triangular channels in PVT systems, which could lead to more efficient and effective energy harvesting from solar radiation in various applications. Shahsavar and Ameri [12] reviewed cooling approaches for photovoltaic thermal systems and emphasised the importance of considering ideal airflow based on ambient and panel temperatures to enhance electrical efficiency. In an experiment, increasing airflow from 0.1 kg/s to 0.3 kg/s improved electrical efficiency. The findings provide valuable insight into optimising airflow in photovoltaic thermal systems for more efficient and effective solar energy systems.

Tahmasbi et al. [13] conducted a numerical simulation study on a rectangular channel with aluminum porous foam to investigate the enhancement of the thermal performance of a photovoltaic panel. The researchers reported that using this design can improve electrical efficiency by 3% Dubey et al. [14] conducted a study to evaluate the performance of a solar photovoltaic module with and without an air channel. The researchers reported that the electrical efficiency for the double glass with a distance along the channel and double glass without a channel is 10.41 and 9.74, respectively In a separate study, Hussain et al. [15] designed hexagonal aluminum channels and placed them under the Tedlar layer to improve the electrical efficiency of a PV. By establishing air flow, the researchers discovered that this design increased the electrical efficiency by 13.7%. These research findings provide valuable insights into the design and optimisation of air channels to improve the performance of photovoltaic modules. Farahani et al. [16] conducted a study on the Rankine cycle, combining a biogas system with a photovoltaic system. Their findings revealed that the presence of the photovoltaic system leads to a

reduction in the overall exergy of the system. Furthermore, they observed that the temperature of the air entering the panel has a transient impact on the radiation received by the Rankine cycle. In their research, Lotfi et al. [17] successfully enhanced the output power of a PV module by 51% through the implementation of water cooling, which effectively lowered the surface temperature from 70 degrees Celsius to 37.5 degrees Celsius. This cooling method not only increased the module's lifespan but also contributed to a reduced energy payback period. Tan et al. [18] conducted an economic and environmental assessment of photovoltaic systems in Hau Giang province. By employing software analysis, they determined that these systems can significantly reduce greenhouse gas emissions, up to 93% when compared to fossil fuel power plants. Additionally, they found that these systems can contribute to the economic prosperity of households. Farahani et al. [19] successfully generated electricity using a (PVT) system by passing air through it and considering the temperature change of the inlet and outlet air. They utilised thermoelectrics and achieved the highest electrical efficiency among (PVT) systems in 9 cities in Iran, with an impressive efficiency of 9.15% in Bojnord. Awda et al. [20] investigated how temperature affects solar panel power output and found that increasing the panel surface temperature from 25 to 70ºC decreased electric power output from 117 to 96.5 W. They concluded that a one-degree Celsius increase in surface temperature results in a 0.48 W decrease in electric power output. These findings provide insight into enhancing solar energy system efficiency. Boussaad et al. [21] investigated the design of a diode circuit with a solar panel and the development of a pulse width modulation (PWM) model. The authors obtained a development model of PWM that was mathematically consistent with the experimental data. This research provides insights into the design and optimisation of circuits for solar panels and the use of PWM techniques for controlling their output. Khodayar Sahebi et al. [22] investigated using mirrors to enhance photovoltaic (PV) system performance and found that placing a mirror next to the PV system increased energy production by 30-70% and lowered the cost of electricity generation by 13%. The research highlights the potential of mirrors as a cost-effective method for enhancing PV system performance. Two ways to increase electrical efficiency are using fluid flow to absorb heat with various geometries, resulting in a 10% increase in electrical efficiency, and using more efficient and expensive MPPT controllers instead of PWM. A systemic view of the entire system is important in evaluating energy and exergy efficiency, considering both thermal and electrical efficiencies and functional wastes. This research highlights the importance of a holistic approach to evaluate the performance of the system.

Jha et al. [23] studied photovoltaic thermal hybrid collectors in North India with two types of absorbers (corrugated and simple). The corrugated absorber plate resulted in lower panel temperature, higher outlet air temperature, and greater overall exergy efficiency. Mittelman et al. [24] studied the relationship between length, depth, Nusselt number, and Rayleigh number in natural convection in a channel behind a vertical flat plate. The authors observed that the channel behind the photovoltaic (PV) panel can increase efficiency by 2% at two specific angles. Bambrook and Sproul [25] conducted research on the impact of air flow rate, channel dimensions, and air thermal resistance on the performance of a solar photovoltaic thermal (PVT) collector, using the dimensionless number of transfer units (NTU). Their findings indicate that these parameters have a significant impact on the performance of the system. Additionally, the authors employed a controller to reduce the amount of electricity required by the fans, which improved the energy efficiency of the PVT collector. Dehghan et al. [26] conducted a study on the cooling of photovoltaic (PV) panels in Zanjan, using two scenarios with 3 and 6 fans and using two types of convergent channels to cool the panel. The convergent channel that diffused air in two directions reduced the panel temperature by up to 8 degrees Celsius. The authors discovered that the scenario with 3 fans was more effective in terms of cooling the PV panels and improving their energy output. This research provides valuable insights into the use of forced convection to enhance the performance of PV panels in hot climates, which could potentially lead to more efficient and effective cooling solutions for PV systems operating in high-temperature environments.

Barone et al. [27] developed a dynamic MATLAB code based on panel tilt parameters, climate conditions, and air velocity. The authors analysed the code by combining photovoltaic (PV) panels and heat pumps in commercial centers and found that the exergy was improved by 4% in the proper conditions due to the passage of air through the panels. This research provides insights into the potential use of dynamic thermal-electrical models to optimise the performance of PV panels and heat pumps in commercial buildings.

Shakouri et al. [28] conducted a comprehensive study on the dynamic simulation of a building-

integrated photovoltaic (BIPV) system, focusing on exergy efficiency, energy efficiency, and energy generated by the photovoltaic system. Their findings indicated that the exergy efficiency of the system is influenced by factors such as cell temperature and solar irradiance

The geometry of photovoltaic-thermal (PVT) systems significantly influences their efficiency and performance. This study focuses on the geometry as a key factor for innovation. While the geometry is designed during static and dynamic flow analyses and cannot be modified as a control variable, it remains the most critical factor impacting overall system performance, including efficiency. Each chosen geometry exhibits unique characteristics in terms of PVT efficiency and performance. This research underscores the importance of geometry optimisation for maximising PVT system performance. To cool photovoltaic (PV) panels, researchers have employed various techniques such as fins, rectangular channels, and convergent channels [29]. Rad et al. [30] conducted research on the cooling of photovoltaic (PV) systems by inducing turbulent air flow in rectangular channels. Their findings indicate that laminar flow is more effective than turbulent flow in PVC channels. The study highlights the importance of selecting an appropriate cooling technique based on the geometry of the PV panel, as their findings suggest that the use of different geometries can have an impact on the electrical efficiency of PV panels. Mustafa et al. [31]. studied the effectiveness of triangular channels that were filled, semi-filled, and empty, when filled with porous metal foam, as a passive cooling system for photovoltaic (PV) modules. The authors discovered that the triangular channel with fully porous foam is the most effective in cooling PV systems. Additionally, they found that porosity near the surface of the panel helps to improve the cooling of the PV module. This research provides valuable insights into the use of passive cooling systems for PV panels and emphasises the importance of porosity in enhancing their cooling efficiency. Amr et al. [32] conducted a study on the use of fin plate heat sinks for cooling photovoltaic (PV) panels. Their findings indicate that an increase in the height and number of fins can reduce the temperature of the PV panel by 5 ºC. However, the authors also observed that increasing the fin thickness did not affect the temperature of the PV panel. Kasaeian et al. [33] presented a model for cooling photovoltaic (PV) panels using both experiments and genetic algorithms. Their experimental system used two PV panels and a copper plate coated with aluminum oxide for improved heat transfer. The walls of the channel are made of polycarbonate glass with a thickness of 4 mm, and the effect of mass flow rate and channel depth was investigated. They found that decreasing the channel depth increased the thermal efficiency by 20% and that both the electrical and thermal efficiency improved as the mass flow rate increased. This research provides insights into the optimal design of cooling channels for PV systems and the importance of considering various parameters.

PV systems can use air to pass through the Tedlar layer from the top/bottom, the glass layer from the top/bottom, or the Trombe wall. Trombe wall increases PV efficiency by decreasing thermal resistance with each rotation due to airflow, while the glass on the Tedlar layer also increases electrical efficiency. Trombe walls can turn buildings into zero-energy buildings [34, 35].

Previous research has primarily used rectangular channels as the cooling geometry for photovoltaic (PV) systems. These findings provide insights into the potential of using various cooling geometries and their impact on the efficiency and performance of PV systems. There are various solutions available for cooling photovoltaic (PV) systems, as shown by previous research. Hussam et al. [36] investigated the performance of a PVT collector with a serpentine flow channel and found that the electrical efficiency can be enhanced by using an inlet air flow rate of 0.02 to 0.03 kg/s. They also reported that the height, length, and number of fins have a significant impact on improving thermal efficiency and reducing pressure drop. Cooling solar panels with airflow can enhance their thermal efficiency by up to 18%. This method is recognised among researchers as one of the most economical, cost-effective, and environmentally friendly cooling approaches. Another such solution is the use of squares, which can reduce the PV temperature by trapping air by about 4ºC to 5ºC [37]. Another method involves passing air through a corrugated or reciprocating channel to cool the PV panels [38].

The geometry of photovoltaic-thermal (PVT) systems is a critical factor affecting their efficiency and performance. In this research, we focus on geometry as the basis of investigation and the primary driver of innovation. While geometry is determined during static and dynamic flow studies and cannot be changed as a control variable during operation, it remains the most important factor influencing all previously mentioned factors, including efficiency. In other words, each chosen geometry offers a specific range of achievable PVT efficiency and performance. This research underlines the significance of geometry

in optimising the performance of PVT systems. To cool photovoltaic (PV) panels, researchers have used various techniques, including fins.

These innovative approaches have shown promise for improving the efficiency and performance of PV systems. Researchers have suggested several techniques, including the use of rectangular channels made from various materials, the combination of fins, and the control of airflow speed. The amount of heating energy collected from the surface of the Tedlar increases as more air flows across it. But none of them considered the spiral geometry which has more efficient performance as dedicated in this research.

By these means, while previous studies have not fully investigated the various aspects of solar panel cooling, this paper examines the energy consumption of different panel components. Using the principles of fluid mechanics and heat transfer, a relationship for cooling a panel with air in a rotating geometry is proposed. To validate this relationship, the TRNSYS software is employed. Furthermore, a dynamic model of the air cooling process for a panel is developed using heat transfer relation analysis in MATLAB.

This research investigates the potential of using spiral geometry for cooling photovoltaic (PV) systems. Static and dynamic modeling are employed to assess system behavior under various conditions. Cooling PV systems is well-established to enhance electrical efficiency. The spiral design extends air residence time within the ducts, facilitating greater heat extraction and leading to increased efficiency. Additionally, the integration of PV-powered cooling fans allows for cooling in remote locations without relying on grid access.

As a technological point of view, The cooling process is significantly affected by various factors, such as temperature difference, fan energy consumption, process duration, and geometry, all of which play a crucial role in determining the amount of heat dissipated. Modifying these factors can help regulate the amount of heat rejected by the system.

2. Static modeling

2.1. Mathematical relations

This research investigated the impact of an absorber on panel temperature and the effect of fan speed control on absorber performance. Euler's equations in polar coordinates were simplified using assumptions to analyse the absorber. Heat transfer equations were then derived for an element of the absorber to establish the relationship between temperature and its performance. The absorbers, made of aluminum air channels with a bow shape, are shown partially in Figure 1 [39], The following assumptions are used to simplify Euler's equations in polar space [40]:

- Air is an incompressible fluid,
- Air is an ideal gas,
- The system is steady state,
- The geometry is symmetrical,
- Pressure changes along the angle are insignificant,
- In the channel, the width is smaller than the length,
- The fan is located at the center of the geometry and the airflow exits at the sides,
- Gravity affects the equations,
- The no-slip condition is applied,
- At the largest radial distance, the airflow is laminar with velocity V,
- The fluid flow is solved in a 2D channel,
- Airflow only enters from the fan side and exits from four directions.

According to Euler's equation, the velocity distribution in the channel can be calculated in the direction of θ, as follows [40]:

$$\rho\left(\frac{\partial u_\theta}{\partial t}+u_r\frac{\partial u_\theta}{\partial r}+\frac{u_\theta}{r}\frac{\partial u_\theta}{\partial \theta}+\frac{u_r u_\theta}{r}\right)=-\frac{1}{r}\frac{\partial P}{\partial \theta}+\rho g_\theta \quad (1)$$

By applying the assumptions, the Euler equation is written in the form of Equation 2 [40]:

$$\frac{\partial u_\theta}{\partial \theta}=0 \quad (2)$$

Equation 1 yields constant velocity (u_θ) inside the channel. To achieve the pressure changes in the direction of θ, it is enough to derive Equation 1 in terms of θ and neglect the movement of the fluid in the radial direction (due to assumption number 6) [40].

$$\frac{\partial P}{\partial \theta}=\frac{\partial(\rho R T_f)}{\partial \theta}=\rho R\frac{\partial T_f}{\partial \theta} \quad (3)$$

Based on the relations, with the placement of numbers, the amount of pressure changes is very

small and is around 2 Pascals and can be ignored. Euler's equation is written in the direction of r as follows [40]:

$$\rho\left(\frac{\partial u_r}{\partial t}+u_r\frac{\partial u_r}{\partial r}+\frac{u_\theta}{r}\frac{\partial u_r}{\partial \theta}-\frac{{u_\theta}^2}{r}+u_z\frac{\partial u_r}{\partial z}\right)=-\frac{\partial P}{\partial r}+\rho g_r \quad (4)$$

Equation 7 is expressed the radial velocity, by using assumptions and boundary conditions, which are written as Equations 5 and 6 [40]:

$$g_r=-g\sin\alpha \quad (5)$$

$$B.C: @r=R_{up}\rightarrow u_r=V \quad (6)$$

In Equations 5 and 6, R_{up} is the highest radial distance of the beginning of the channels from the suction port, and α is the slope of the panel. A portion of the geometry under consideration is shown in Figure 1. The dimensions of the elements, including the radius and thickness, are also specified in the same Figure.

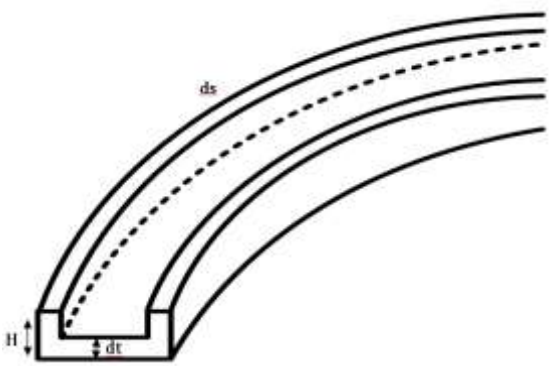

Figure 1. Bow-shaped channel [39]

$$u_r=-\sqrt{-2\left[u_\theta^2\ln\frac{R_{down}}{R_{up}}+g\left(R_{down}-R_{up}\right)\right]+V^2} \quad (7)$$

In Equation (7), the minus sign arises because the direction of the velocity is opposite to the direction of the radial coordinate, r. By applying Euler's equation in the effective zone of the fan, the velocity distribution at the center of the absorber can also be obtained. It is important to note that the speed in the z-direction is considered constant, which corresponds to the output speed of the fan. We can denote this constant speed as h within the formulas [40].

$$\rho\left(\frac{\partial u_z}{\partial t}+u_r\frac{\partial u_z}{\partial r}+\frac{u_\theta}{r}\frac{\partial u_z}{\partial \theta}+u_z\frac{\partial u_z}{\partial z}\right)=-\frac{\partial P}{\partial z}+\rho g_z \quad (8)$$

By solving Equation 8, pressure changes in the z-direction are calculated as follows [40]:

$$\Delta P=\rho g h\cos\alpha \quad (9)$$

Equation (9) defines h as the height from the system floor to the fan. We revisit Equation (1) to obtain the velocity along the radius in this zone. However, here, the velocity varies with height along the r-direction. For this zone, we neglect movement in the θ-direction and pressure drop. Therefore, Equation 10 is expressed as follows:

$$\rho u_z\frac{\partial u_r}{\partial z}=-\rho g\sin\alpha \quad (10)$$

According to the mentioned points, Considering Equations 7 and 10, simultaneously resulted in Equation 11 can be written as follows:

$$\frac{g\sin\alpha}{v_{fan}}(h)=-\sqrt{-2\left[u_\theta^2\ln\frac{R_{down}}{R_{up}}+g\left(R_{down}-R_{up}\right)\right]+V^2} \quad (11)$$

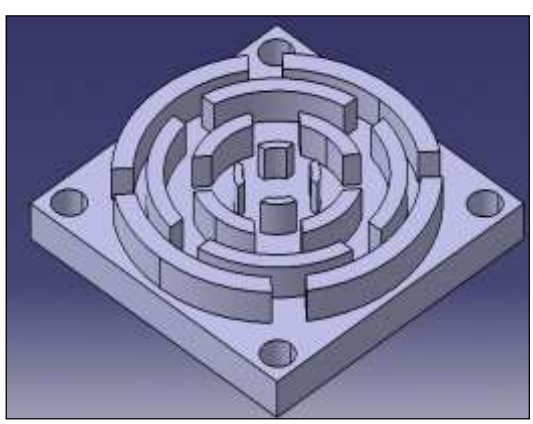

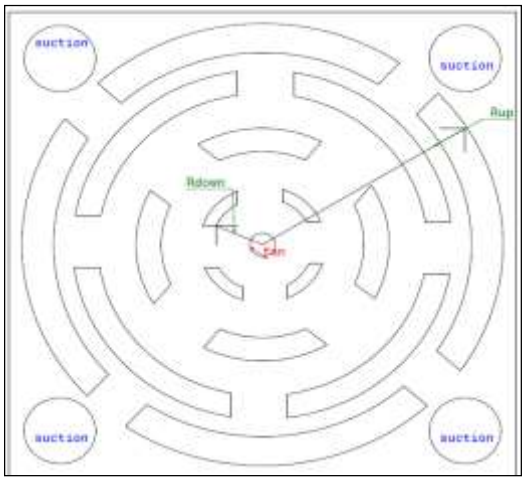

Figure 2. General view of channels and suction part and fan zone

Continuity equations are used to calculate the fan speed. Solving Equations 13 and 14 allows us to calculate the velocity inside the channel. A control volume between the suction port and the fan output zone is considered, and the steady state continuity equation is applied to it. The fan and suction part are positioned according to the desired geometry in Figure 2. In Figure 2, the directions of the inlet and outlet airflows are indicated [40].

$$\dot{m}_{in} - \dot{m}_{out} = 0 \quad (12)$$

The equation shows m_{in} and m_{out} are input/output mass flow rates, related to suction and input channels/fan output, respectively.

$$\dot{m}_{in} = \rho A_P V \quad (13)$$

$$\dot{m}_{out} = \rho A_{fan} v_{fan} + n\rho A_{duct} u_\theta \quad (14)$$

By combining Equation 12 with Equation 14, the inlet channel velocity and the suction velocity are calculated as follows:

$$\frac{g\sin\alpha}{v_{fan}}(h) = \sqrt{-2\left[u_\theta^2 \ln\frac{R_{down}}{R_{up}} + g\left(R_{down} - R_{up}\right)\right] + \left(\frac{A_{fan}v_{fan} + nA_{duct}u_\theta}{A_P}\right)^2} \quad (15)$$

By sorting and standardisation of Equation 15, a quadratic equation is achieved in terms u_θ as expressed in Equation 16:

$$\left(-2\ln\frac{R_{down}}{R_{up}} + \frac{n^2A_{duct}^2}{A_P^2}\right)u_\theta^2 + 2\frac{A_{fan}A_{duct}}{A_P} n v_f u_\theta + \left(\frac{A_{fan}^2 v_{fan}^2}{A_p^2} - 2g\left(R_{down} - R_{up}\right) - \frac{g^2\sin^2\alpha h^2}{v^2_{fan}}\right) = 0 \quad (16)$$

Equation 17 expresses the quadratic equation in standard form from Equation 16. The coefficients a, b, and c in Equation 17 define the quadratic equation [40].

$$au_\theta^2 + bu_\theta + c = 0 \quad (17)$$

$$u_\theta = \frac{-b + \sqrt{b^2 - 4ac}}{2a} \quad (18)$$

$$a = -2\ln\frac{R_{down}}{R_{up}} + \frac{n^2A_{duct}^2}{A_P^2} \quad (19)$$

$$b = 2\frac{A_{fan}A_{duct}}{A_P} n v_f \quad (20)$$

$$c = \frac{A_{fan}^2 v_{fan}^2}{A_p^2} - 2g\left(R_{down} - R_{up}\right) - \frac{g^2\sin^2\alpha h^2}{v^2_{fan}} \quad (21)$$

The suction velocity of the fan in Equation 22 is expressed as:

$$V = \frac{A_{fan}v_{fan} + nA_{duct}\left(\frac{-b + \sqrt{b^2 - 4ac}}{2a}\right)}{A_P} \quad (22)$$

The absorber temperature in the panel was calculated using the input/output energy balance shown in Figure 3. A U-shaped duct is considered based on the front view. For ease of calculation, this duct can be expanded as shown in Figure 3.

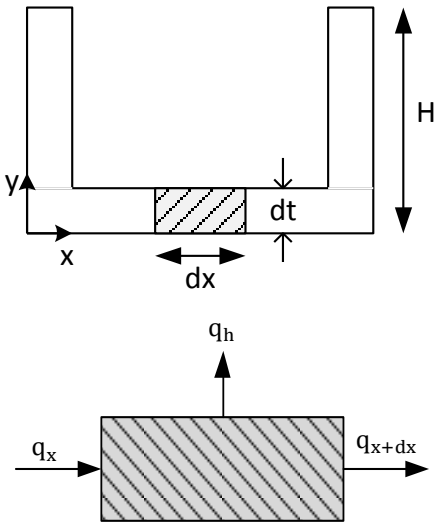

Figure 3. Input and output energy to the element [41]

In Figure 3, q_x and q_{x+dx} are input and output conductive heat transfer to the element, respectively. q_h is the convective heat transfer between the air inside the channel and Tedlar. By calculating the values and simplifying, 2nd order linear differential equation is obtained with 22 constant coefficients [41].

$$k_d dt.\frac{\partial^2 T}{\partial x^2} - h_f(T(x) - T_f) = 0 \quad (23)$$

Boundary conditions are written as Equations 24 and 25 are used in Equation 23 [41].

$$B.C.: \begin{cases} @x = 0 & : T = T_{tedlar} \\ @x = l: T = T_{tedlar} \end{cases} \quad (24)$$

$$m^2 = \frac{h_f}{k_d dt} \quad (25)$$

By applying the boundary conditions, the absorber temperature is defined as Equation 26:

$$T(x) = \frac{(T_{tedlar} - T_f)}{sinhml}(sinhm(l - x) + sinhmx) + T_f \quad (26)$$

The channel temperature distribution function is calculated. for ease of calculations, the average of this function can be acquired by Lagrange's theorem. Equation 27, T_U means the average temperature of the U-shaped duct [41].

$$T_U = \frac{2(T_{Tedlar} - T_f)}{mlsinhml}(coshml - 1) + T_f \quad (27)$$

As shown in Figure 4 Fluid element was chosen as the control volume, and rules were applied.

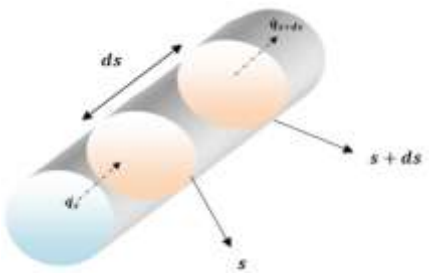

Figure 4. Fluid elements inside the channel [41]

The energy received by the fluid from the plates of the U-shaped duct and the Tdlar is equal to the rate at which thermal energy changes between sections s and s+ds. The heat input for sound control is q_s˙, while the heat output is q˙_(s+ds). The fluid receives energy from the pedlar and the U-shaped channel [41].

$$h_f T_t = \frac{\dot{m}c}{l}\frac{\partial T_f}{\partial s} + h_f(2T_f - T_U) \quad (28)$$

Lagrange's theorem calculates the average channel temperature via Equation 29 [42].

$$\overline{T}_f(\theta) = T_t + \frac{T_t - T_{in}}{rU\theta}(e^{-rU\theta} - 1) \quad (29)$$

Equations 30 and 31 define the 5-parameter solar cell model [43].

$$I = I_L - I_o\left[\exp\left(\frac{V + IR_s}{a}\right) - 1\right] - \frac{V + IR_s}{R_{sh}} \quad (30)$$

$$a = \gamma k T_{cell}/q \quad (31)$$

2.2. The static model solving

To solve the problem using a static approach, the fixed parameters listed in Table 1 are required. Subsequently, a system of three differential equations, representing cell, glass, and Tedlar temperatures, was solved using the FDM since there is no analytical solution due to its nonlinear nature. Newton's method was used to bring all terms to one side and solve for the system, with initial assumptions of all temperatures equaling 310 K [41].

Table 1. Constant values in the electrical model [44]

parameters	Amounts
$\eta_{el,ref}$	0.1306
$I_{sc,ref}$	3.66 A
$V_{oc,ref}$	22.1 V
$I_{mp,ref}$	3.28 A
$V_{mp,ref}$	18.3 V
$T_{cell,ref}$	25℃

3. Dynamic modeling

3.1. Dynamic analysis

As shown in Figure 5, the solar panel consists of the following parts: glass, Tedlar, cells, and absorbers. To solve the heat transfer relations, each section is considered a control volume, and the heat transfer relations are written for them. To simplify the problem, assumptions 7 to 10 are used [41].

- A glass cover is thin, and one-dimensional heat transfer is assumed.
- The reflection coefficient for glass is omitted.
- The reflection and absorption coefficient for the cell are ignored.
- The same ambient temperature around the system
- There is no airflow passage beside the panel.
- In radiative equations, the sky is assumed to be a black body.

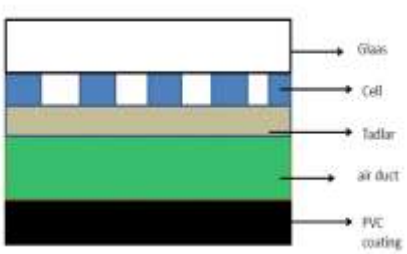

Figure 5. Components of a PV/T system Glass

3.1.1. Glass

As shown in Figure 6 Energy entering glass equals solar irradiation per unit area. Radiant heat transfer from the glass to the sky, convective heat transfer from the glass to the surrounding environment, and conductive heat transfer from the glass to the solar cell make up the emitted energies. Equation 32 is derived from thermal control volume [45, 46].

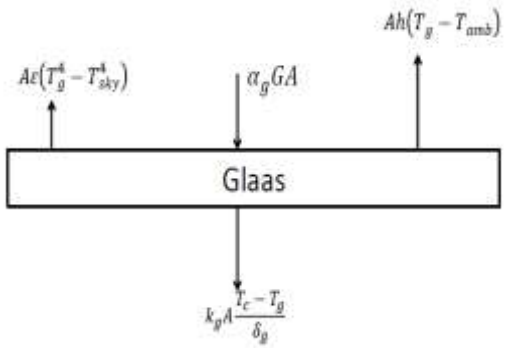

Figure 6. Control volume for glass

$$\alpha_g GA - A\varepsilon\left(T_g^4 - T_{sky}^4\right) - Ah\left(T_g - T_{amb}\right) - k_g A\frac{T_c - T_g}{\delta_g} = (\rho c_p)_g A\delta_g\frac{\partial T_g}{\partial t} \quad (32)$$

3.1.2. Cell

In the control volume shown in Figure 7, energy entering the cell equals conductive heat transfer between the cell and glass plus radiation passing through the glass. Outgoing energies are radiant heat transfer between cell and sky and conductive heat transfer between Tedlar and cell. Equation 33 applies the control volume on the cell [40].

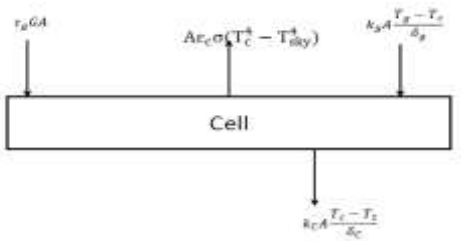

Figure 7. Control volume for the cel

$$\tau_g GA - k_C A\frac{T_c - T_t}{\delta_C} + k_g A\frac{T_g - T_c}{\delta_g} - A\varepsilon_c\sigma(T_c^4 - T_{sky}^4) = (\rho c_p)_c A\delta_c\frac{\partial T_c}{\partial t} \quad (33)$$

3.1.3. Tadlar

Energy entering Tedlar is conductive heat transfer between Tedlar and cell, while energy leaving Tedlar is heat transfer between Tedlar and the surrounding environment**.** Energy exchange in dollars can be observed in a figure 8 pattern [40].

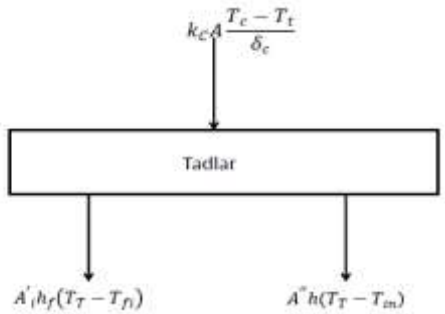

Figure 8. Control volume for Tadlar with absorbe

$$k_C A\frac{T_c - T_t}{\delta_c} - Ah(T_t - T_{amb}) = (\rho c_p)_t A\delta_t\frac{\partial T_t}{\partial t} \quad (34)$$

According to Equations 32 to 34, three unknowns T_{cell}, T_{tedlar}, $T_{Glass}$are obtained. MATLAB software was used to solve this system with three equations with three unknowns.

3.2. The dynamic model solution

According to Equations 32 to 34, a differential equation system has been formed, and the Finite Difference Method (FDM) has been used to solve it. Then Equations 35 to 37 are achieved based on the time derivative. In equations, 35 to 37, Δt represents the time interval between measurements. Smaller values of Δt lead to more accurate responses with less error. The results of the static analysis were used as initial assumptions in MATLAB to calculate responses at different times. In dynamic modeling, a fixed time interval of 5 minutes was used to extract the results [47].

$$T_g^{t+1} = \frac{\Delta t}{(\rho c_p)_g \delta_g}\left[\alpha_g G - \varepsilon\left((T_g^{\,4})^t - T_{sky}^4\right) - h\left(T_g^{\,t} - T_{amb}\right) - k_g\frac{T_c^{\,t} - T_g^{\,t}}{\delta_g}\right] + T_g^{\,t} \quad (35)$$

$$T_c^{t+1} = \frac{\Delta t}{(\rho c_p)_c \delta_c}\left[\tau_g G - k_C\frac{T_c - T_t}{\delta_C} + k_g\frac{T_g - T_c}{\delta_g} - \varepsilon_c\sigma(T_c^4 - T_{sky}^4)\right] + T_c^{\,t} \quad (36)$$

$$T_t^{t+1} = \frac{\Delta t}{(\rho c_p)_t \delta_t}\left[k_C\frac{T_c - T_t}{\delta_c} - h(T_t - T_{amb}))\right] + T_t^{\,t} \quad (37)$$

Table 2. Fixed parameters in modeling [44]

parameters	Amounts
NOCT	47(℃)
α_{Glass}	0.066
k_{Glass}	0.93(W.M-1.K-1)
ε	0.83
τ_{glass}	0.88
δ_{Glass}	0.003 (M)
δ_{cell}	0.002 (M)
k_{cell}	273 (W.M-1.K-1)
ε_c	0.95
A'_i	0.300 (M^2)
A''	0.136 (M^2)
θ	110°
L_0	0.215 (M)
H	5 (Cm)
dt	1 (Cm)
k_d	300 (W.M-1.K-1)
ρ_{air}	1.4 (Kg.M-3)
R_{air}	0.287 (Kj.Kg-1.K-1)
g	9.81(M.S-2)
α	33°
μ_{air}	10-6 (N.S.M-2)

4. Results

4.1. Static model results

The experimental results were analysed by investigating the static state using the output current-voltage diagram from the panel and analysing static relations. Static conditions differ from dynamic conditions due to constant irradiation and environmental conditions that do not change over time. Equation 29 was used to obtain the current-voltage curve without a heat absorber, with an irradiation of 800 (W/m^2), an ambient temperature of 30ºC, and a cell temperature of 48ºC. As shown in Figure 9, The PV had an open circuit voltage of 23.48 (V) and a short circuit current of 2.8 (A). A thermal absorber was then installed. Static modeling and constant environmental conditions show a 7°C decrease in panel temperature with a thermal absorber. As shown in Figure 10, The panel's power increased by 3.8%, while cell temperature decreased by 17%. The maximum voltage and power values of the solar panel are shown in Figures 9 and 10.

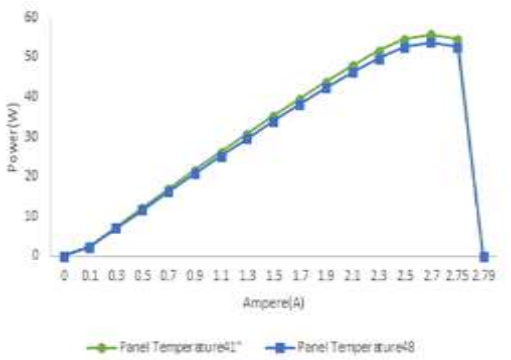

Figure 9. Diagram of power and output current of the panel with and without absorber

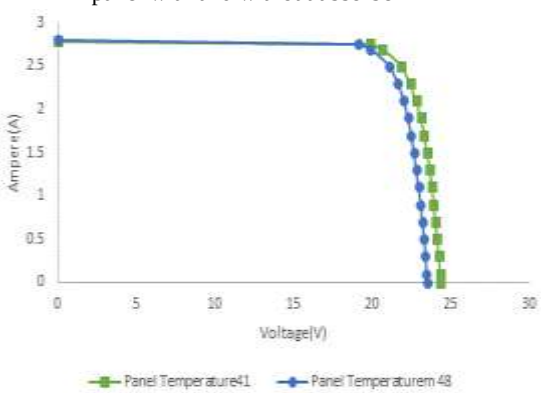

Figure 10. Voltage-current diagram with and without absorber

4.2. Dynamic model results

Modeling is done for peak sunlight hours, 10 AM-to 5 PM. The average temperature in the summer was 37ºC. The modeling was carried out for Karaj, which has a latitude of 35 degrees and a longitude of 51 degrees [48]**.** The panel temperature reaches 1.5 times the ambient temperature, and Panel power decreases as the panel temperature increases, especially when the temperature rises significantly. One available solution is to use a thermal absorber, which can reduce the panel temperature by 8%. As shown in Figure 11, This thermal absorber passively repels heat transfer. In this research, it is assumed that solar noon time is 13:00. At 10:00 A.M., the input irradiation is 600 and 900 (W/m2). The cell temperature with the absorber increases more than in the morning due to the efficiency of the absorber. The difference in area temperature with and without absorber reaches 16.8ºC before noon. In other words, when the solar irradiation reaches a peak, the absorber can cool down by about 16.8ºC. As can be seen in Figure 11, the presence of an absorber can cause a change of about 15 degrees Celsius in the panel temperature.

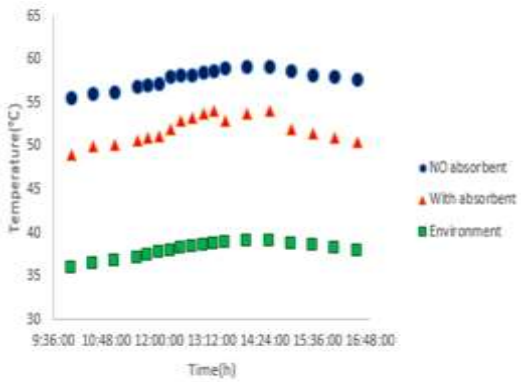

Figure 11. cell and ambient temperature comparison

As shown in Figure 12, in the hottest state of the system, the thermal absorber was able to lower the cell temperature by approximately 5ºC, which is equivalent to an increase of about 2% in electrical efficiency. At 13:00, when the panel receives maximum irradiation, the panel temperature rises, and the absorber starts working. On average, the system with the absorber was able to add 12.55 volts to the battery voltage, while without the absorber, the average number was 12.51 volts. Modeling voltage without the absorber from 10:00 A.M. to 1:00 P.M. (solar noon) differed from the measured value The importance of the damper can be seen in Figure 12.

The modified damper can transfer more energy to the battery.

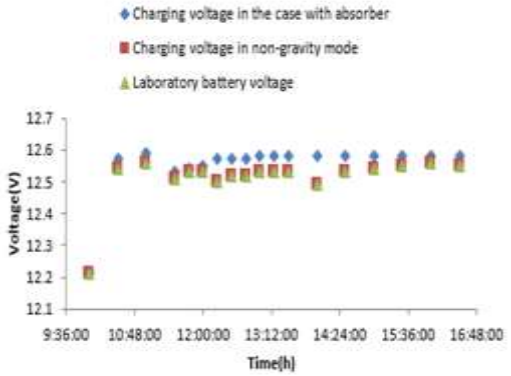

Figure 12. 65 amp-hour battery charging diagram on the day of the test with and without thermal absorber

4.3. Evaluation of results

To evaluate the results, a PV/T system was also simulated in two open-source code software and was calculated using Equation 38. Equation 38 uses $X_{sim,i}$ for modeling, and $X_{TRNS,i}$ for TRNSYS software, with n as the data number. A PV/T system with a 60 W panel was compared using TRNSYS software, and results were compared to Table 3, showing an RMSPR of 1.2%, indicating an acceptable agreement between the results of these two approaches [44].

$$RMS = \sqrt{\frac{\sum \left[100 \times \frac{X_{sim,i} - X_{TRNS,i}}{X_{TRNS,i}}\right]^2}{n}} \quad (38)$$

Table 3. Comparison and validation of TRNSYS output and modeling

TRNSYS software output			Modeling output		
Voltage (v)	Ampere (A)	Power (W)	Voltage (v)	Ampere (A)	Power (W)
25	0	0.00	24.36	0.00	0.00
24.94	0.1	2.49	24.32	0.10	2.43
24.87	0.3	7.46	24.23	0.30	7.27
24.8	0.5	12.40	24.14	0.50	12.07
24.71	0.7	17.30	24.03	0.70	16.82
24.6	0.9	22.14	23.92	0.90	21.53
24.3	1.1	26.73	23.80	1.10	26.18
24.16	1.3	31.41	23.66	1.30	30.76
24.02	1.5	36.03	23.50	1.50	35.25
23.8	1.7	40.46	23.31	1.70	39.63
23.61	1.9	44.86	23.09	1.90	43.86
23.3	2.1	48.93	22.80	2.10	47.89
22.74	2.3	52.30	22.43	2.30	51.58
22.09	2.5	55.23	21.86	2.50	54.64
20.86	2.7	56.32	20.63	2.70	55.69
19.94	2.75	54.84	19.85	2.75	54.59
0	2.8	0.00	0.00	2.79	0.00

5. Conclusions

This study investigated the use of spiral geometry as an absorber using MATLAB software for both static and dynamic modeling, including equation solving. The dynamic simulation employed both first-order and nonlinear partial differential equations. The numerical simulation utilised a fixed time step of 5 minutes, with the integral of the derivatives estimated using the area under the curve method. Following the dynamic simulation, the system's electrical behavior was analysed, focusing on how temperature reduction affects the output voltage and current from the panel, the battery input, and the load. The study assumed an ambient temperature of 35°C and examined the energy balance. The results indicated that the absorber performed effectively when the temperature remained below the design point ambient temperature. In conclusion, the study evaluated the system's performance at high and low temperatures under both static and dynamic conditions. The study conducted dynamic modeling of the flow at a lower ambient temperature, i.e. 34°C, resulting in a cell temperature of 58.5°C without the absorber and 53°C with the absorber. The electrical efficiency was found to be 7.4% without the absorber and 9.2% with the absorber. According to the outcome of the static flow modeling, the absorber's electrical efficiency can range from 7.5% to 10% in environments where the temperature is below 35°C (i.e., 33°C). By applying the static model absorber, the cell temperature decreased from 58°C to 52°C.

6. Future works

In the study, a spiral geometry having four radii was analysed, and it was recommended that future work explore a new geometry with a larger radius for better performance under higher temperatures. Further investigation will focus on pressure drop, entropy, and system performance to contribute to current research in this field. In addition to extending the lifespan of solar panels, cooling them can also significantly improve their electrical efficiency.

Among the various cooling methods, air cooling has become widespread due to its low cost and ease of implementation. However, the inherent specific heat of the air and its low thermal conductivity prevent ideal cooling of the panels. In this context, the development of novel geometries emerges as an innovative approach to overcome this challenge. By optimising the panel structure and employing creative geometries, airflow can be guided more effectively and heat loss can be minimised. The widespread adoption of these novel geometries has the potential to significantly enhance the electrical efficiency of solar panels. This plays a crucial role in promoting sustainable development and reducing reliance on fossil fuels.

Acknowledgment

This work was supported by the Materials and Energy Research Center (MERC) under Grant 521393001.

Nomenclature

A	Photovoltaic cell area[m^2]
A'_i	Total area of the T_{tedlar} and the air channel [m^2]
A"	Total area of the inlet duct and the T_{tedlar} [m^2]
A_{duct}	Duct area [m^2]
C_p	Specific heat of air [$J.kg^{-1}.K^{-1}$]
G	Solar irradiance [$W.m^{-2}$]
g	Gravitational acceleration [$m.s^{-2}$]
H f	Heat transfer coefficient (fluid convection): [$W.m^{-2}.K^{-1}$]
h	Heat transfer coefficient (convection): [$W.m^{-2}.K^{-1}$]
I d	Short-circuit diode current: [A]
I out	Output current: [A]
I s c	Short-circuit current [A]
J	Jacobi matrix
K cell	Conductivity of the cell [$W.m^{-1}.K^{-1}$]
K Glass	Conductivity of glass [$W.m^{-1}.K^{-1}$]
K d	Heat transfer coefficient (conduction) [$W.m^{-1}.K^{-1}$]
L	Length of the channel [m]
L0	Length of the channel [m]
m ̈in	Inlet mass flow rate [$kg.s^{-1}$]
NOCT [K]	Nominal operating cell temperature
P	Pressure: [Pa]
Pout	Output electric power [W]
R s h	Shunt resistance [Ω]
R s	Series resistance [Ω]
R_{up}	The highest radial distance of the beginning of the channels from the suction part [m]
R_{down}	The lowest radial distance of the beginning of the channels from the suction part[m]
T_{amb}	Ambient temperature [K]
T cell	Solar cell temperature [K]
T Glass	Temperature of the glass: [K]
Tin	Inlet fluid temperature [K]
U r	Radial velocity [$m.s^{-1}$]
u_θ	Radial velocity [$m.s^{-1}$]
V	Duct velocity [$m.s^{-1}$]
V out	Output voltage [V]
D t	Width of the channel [m]
q s ̇	Volume heat generation rate [$W.m^{-3}$]

Greek letters

α	Coefficient of thermal expansion: [K-1]
α_Glass	Heat transfer coefficient [$W.m^{-2}.K^{-1}$]
β	Voltage coefficient
Δ cell	Thickness of the cell [m]
δ Glass	Thickness of the glass [m]
ε	Heat transfer coefficient (glass emission) [$W.m^{-2}.K^{-4}$]
η	Panel efficiency
μ	Viscosity of air [Pa. s]
τ glass	Heat transfer coefficient (glass transmission)
ρ	Density of air [$kg.m^{-3}$]

Subscripts

a	Amb
C	cell
f	fan
d	duct
G	Glass
In	inlet
Out	outlet
Sc	Short-circuit
s	sky
T	Tedlar

References

[1] S. Abdul Hamid, M. Yusof Othman, K. Sopian, and S. H. Zaidi, "An overview of photovoltaic thermal combination (PV/T combi) technology," *Renewable and Sustainable Energy Reviews,* vol. 38, pp. 212-222, 2014/10/01/ 2014. doi:https://doi.org/10.1016/j.rser.2014.05.083.

[2] K. Anshu, P. Kumar, and B. Pradhan, "Numerical simulation of stand-alone photovoltaic integrated with earth to air heat exchanger for space heating/cooling of a residential building," *Renewable Energy,* vol. 203, pp. 763-778, 2023/02/01/ 2023. doi:https://doi.org/10.1016/j.renene.2022.12.081

[3] E. Cuce, T. Bali, and S. A. Sekucoglu, "Effects of passive cooling on performance of silicon photovoltaic cells," *International Journal of Low-Carbon Technologies,* vol. 6, pp. 299-308, 2011. doi: 10.1093/ijlct/ctr018.

[4] B. J. Brinkworth and M. Sandberg, "Design procedure for cooling ducts to minimise efficiency loss due to temperature rise in PV arrays," *Solar Energy,* vol. 80, pp. 89-103, 2006/01/01/ 2006. doi:10.1016/j.solener.2005.05.020.

[5] R. Mazón-Hernández, J. R. García-Cascales, F. Vera-García, A. S. Káiser, and B. Zamora, "Improving the Electrical Parameters of a Photovoltaic Panel by Means of an Induced or Forced Air Stream," *International Journal of Photoenergy,* vol. 2013, p. 830968, 2013/03/30 2013. doi: 10.1155/2013/830968.

[6] A. N. Özakin and F. Kaya, "Effect on the exergy of the PVT system of fins added to an air-cooled channel: A study on temperature and air velocity with ANSYS Fluent," *Solar Energy,* vol. 184, pp. 561-569, 2019/05/15/ 2019. doi: 10.1016/j.solener.2019.03.100.

[7] K. Sopian, K. S. Yigit, H. T. Liu, S. Kakaç, and T. N. Veziroglu, "Performance analysis of photovoltaic thermal air heaters," *Energy Conversion and Management,* vol. 37, pp. 1657-1670, 1996/11/01/ 1996doi: https://doi.org/10.1016/0196-8904(96)00010-6

[8] A. Almuwailhi and O. Zeitoun, "Investigating the cooling of solar photovoltaic modules under the conditions of Riyadh," *Journal of King Saud University - Engineering Sciences,* vol. 35, pp. 123-136, 2023/02/01/ 2023. doi: https://doi.org/10.1016/j.jksues.2021.03.007

[9] H. Vajedi, M. Dehghan, M. Aminy, A. Pourrajabian, and G. Gediz Ilis, "Experimental study on an air-based photovoltaic-thermal (PV-T) system with a converging thermal collector geometry: A comparative performance analysis," *Sustainable Energy Technologies and Assessments,* vol. 52, p. 102153, 2022/08/01/ 2022 doi: 10.1016/j.seta.2022.102153.

[10] S. Irfan Sadaq, S. Nawazish Mehdi, and M. Mohinoddin, "Experimental analysis on solar photovoltaic (SPV) panel for diverse slope angles at different wind speeds," *Materials Today: Proceedings,* 2023/04/25/ 2023. doi: https://doi.org/10.1016/j.matpr.2023.04.265

[11] M. Y. H. OTHMAN and H. Ruslan, "Kajian Prestasi Pengumpul Suria Fotovoltan-Terma (Pv/T) dengan Plat Penyerap Lengkuk-V," *Sains Malaysiana,* vol. 38, pp. 537-541, 2009.

[12] A. Shahsavar and M. Ameri, "Experimental investigation and modeling of a direct-coupled PV/T air collector," *Solar Energy,* vol. 84, pp. 1938-1958, 2010/11/01/ 2010. doi: 10.1016/j.solener.2010.07.010.

[13] M. Tahmasbi, M. Siavashi, A. M. Norouzi, and M. H. Doranehgard, "Thermal and electrical efficiencies enhancement of a solar photovoltaic-thermal/air system (PVT/air) using metal foams," *Journal of the Taiwan Institute of Chemical Engineers,* vol. 124, pp. 276-289, 2021/07/01/ 2021. doi:https://doi.org/10.1016/j.jtice.2021.03.045

[14] S. Dubey, G. S. Sandhu, and G. N. Tiwari, "Analytical expression for electrical efficiency of PV/T hybrid air collector," *Applied Energy,* vol. 86, pp. 697-705, 2009/05/01/ 2009. doi:https://doi.org/10.1016/j.apenergy.2008.09.003.

[15] F. Hussain, M. Y. H. Othman, K. Sopian, B. Yatim, H. Ruslan, and H. Othman, "Design development and performance evaluation of photovoltaic/thermal (PV/T) air base solar collector," *Renewable and Sustainable Energy Reviews,* vol. 25, pp. 431-441, 2013/09/01/ 2013. doi:https://doi.org/10.1016/j.rser.2013.04.014.

[16] S. D. Farahani, M. Borzabadi Farahani, and A. Sajedi, "Thermodynamic Analysis of ORC-GT Hybrid Cycle and Thermal Recovery from Photovoltaic Panels," *Journal of Solar Energy Research,* vol. 7, pp. 1198-1210, 2022. doi: 10.22059/jser.2022.325213.1206.

[17] M. Lotfi, A. H. Shiravi, T. Bahrami, and M. Firoozzadeh, "Cooling of PV Modules by Water, Ethylene-Glycol and Their Combination; Energy and Environmental Evaluation," *Journal of Solar Energy Research,* vol. 7, pp. 1047-1055, 2022. doi: 10.22059/jser.2022.327060.1228.

[18] T. V. Tan and L. T. Cao, "Evaluating the rooftop solar photovoltaic potential in Hau Giang province," *Journal of Solar Energy Research,* vol. 6, pp. 751-760, 2021. doi: 10.22059/jser.2021.322150.1200.

[19] s. d. Farahani and M. Alibeigi, "Investigation of power generated from a PVT-TEG system in Iranian cities," *Journal of Solar Energy Research,* vol. 5, pp. 603-616, 2020. doi: 10.22059/jser.2020.308162.1170.

[20] L. Awda, Y. Khalaf, and S. Salih, "Analysis of Temperature Effect on a Crystalline Silicon Photovoltaic Module Performance," *International Journal of Engineering,* vol. 29, pp. 722-727, 2016. https://www.ije.ir/article_72728.html.

[21] M. Boussaada, R. Abdelaati, and H. Yahia, "Emulation, Model Identification and New-approach Characterization of a PV Panel

(TECHNICAL NOTE)," *International Journal of Engineering*, vol. 31, pp. 1222-1227, 2018. doi: 10.5829/ije.2018.31.08b.09.

[22] H. Khodayar Sahebi, S. Hoseinzadeh, H. Ghadamian, M. H. Ghasemi, F. Esmaeilion, and D. A. Garcia, "Techno-economic analysis and new design of a photovoltaic power plant by a direct radiation amplification system," *Sustainability*, vol. 13, p. 11493, 2021. doi: 10.3390/su132011493.

[23] P. Jha, B. Das, and R. Gupta, "Performance of air-based photovoltaic thermal collector with fully and partially covered photovoltaic module," *Applied Thermal Engineering*, vol. 180, p. 115838, 2020/11/05/ 2020. doi:https://doi.org/10.1016/j.applthermaleng.2020.11 5838.

[24] G. Mittelman, A. Alshare, and J. H. Davidson, "A model and heat transfer correlation for rooftop integrated photovoltaics with a passive air cooling channel," *Solar Energy*, vol. 83, pp. 1150-1160, 2009/08/01/ 2009. doi: https://doi.org/10.1016/j.solener.2009.01.015

[25] S. M. Bambrook and A. B. Sproul, "Maximising the energy output of a PVT air system," *Solar Energy*, vol. 86, pp. 1857-1871, 2012/06/01/ 2012. doi: https://doi.org/10.1016/j.solener.2012.02.038.

[26] M. Dehghan, S. Rahgozar, A. Pourrajabian, M. Aminy, and F.-S. Halek, "Techno-economic perspectives of the temperature management of photovoltaic (PV) power plants: A case-study in Iran," *Sustainable Energy Technologies and Assessments*, vol. 45, p. 101133, 2021/06/01/ 2021. doi: https://doi.org/10.1016/j.seta.2021.101133.

[27] G. Barone, A. Buonomano, C. Forzano, A. Palombo, and O. Panagopoulos, "Experimentation, modelling and applications of a novel low-cost air-based photovoltaic thermal collector prototype," *Energy Conversion and Management*, vol. 195, pp. 1079-1097, 2019. doi: 10.1016/j.enconman.2019.04.082.

[28] M. Shakouri, H. Ghadamian, and A. Noorpoor, "Energy and Exergy Quasi-Dynamic Analysis of Building Integrated Photovoltaic System Using Data Analytics," *Journal of Solar Energy Research*, vol. 4, pp. 273-279, 2019. doi: 10.22059/jser.2020.295324.1136

[29] A. A. B. Baloch, H. M. S. Bahaidarah, P. Gandhidasan, and F. A. Al-Sulaiman, "Experimental and numerical performance analysis of a converging channel heat exchanger for PV cooling," *Energy Conversion and Management*, vol. 103, pp. 14-27, 2015/10/01/ 2015. , doi: 10.1016/j.enconman.2015.06.018

[30] A. Hosseini Rad, H. Ghadamian, H. R. Haghgou, and F. Sarhadi, "Energy and exergy evaluation of multi-channel photovoltaic/thermal hybrid system: simulation and experiment," *International Journal of Engineering*, vol. 32, pp. 1665-1680, 2019. .doi: 10.5829/IJE.2019.32.11A.18

[31] J. Mustafa, S. Alqaed, and M. Sharifpur, "Enhancing the energy and exergy performance of a photovoltaic thermal system with ∇-shape collector using porous metal foam," *Journal of Cleaner Production*, vol. 368, p. 133121, 2022/09/25/ 2022. https://doi.org/10.1016/j.jclepro.2022.133121.

[32] A. A.-r. Amr, A. A. M. Hassan, M. Abdel-Salam, and A. M. El-Sayed, "Enhancement of photovoltaic system performance via passive cooling: Theory versus experiment," *Renewable Energy*, vol. 140, pp. 88-103, 2019/09/01/ 2019. doi:https://doi.org/10.1016/j.renene.2019.03.048

[33] A. Kasaeian, Y. Khanjari, S. Golzari, O. Mahian, and S. Wongwises, "Effects of forced convection on the performance of a photovoltaic thermal system: An experimental study," *Experimental Thermal and Fluid Science*, vol. 85, pp. 13-21, 2017/07/01/ 2017. doi: 10.1016/j.expthermflusci.2017.02.012.

[34M. Hemmat Esfe, M. H. Kamyab, and M. Valadkhani, "Application of nanofluids and fluids in photovoltaic thermal system: An updated review," *Solar Energy*, vol. 199, pp. 796-818, 2020/03/15/ 2020. doi: 10.1016/j.solener.2020.01.015.

[35] Y. Abdalgadir, H. Qian, D. Zhao, A. Adam, and W. Liang, "Daily and annual performance analyses of the BIPV/T system in typical cities of Sudan," *Energy and Built Environment*, vol. 4, pp. 516-529, 2023/10/01/ 2023. doi: 10.1016/j.solener.2020.01.015.

[36] W. K. Hussam, A. M. Khlefat, and G. J. Sheard, "Energy saving and performance analysis of air‐cooled photovoltaic panels," *International Journal of Energy Research*, vol. 46, pp. 4825-4834, 2022. doi: 10.1002/er.7475

[37] Y. Yektaeian, N. Bahraminezhad, and S. Yazdani, "Feasibility PV Integration in Trombe Wall for Iran Climates," *Journal of Solar Energy Research*, vol. 2, pp. 59-64, 2017. Available: https://jser.ut.ac.ir/article_63945.html.

[38] A. Ibrahim, M. Y. Othman, M. H. Ruslan, S. Mat, and K. Sopian, "Recent advances in flat plate photovoltaic/thermal (PV/T) solar collectors," *Renewable and Sustainable Energy Reviews*, vol. 15, pp. 352-365, 2011/01/01/ 2011. , doi: 10.1016/j.rser.2010.09.024.

[39] M. Herrando, K. Wang, G. Huang, T. Otanicar, O. B. Mousa, R. A. Agathokleous, Y. Ding, S.

Kalogirou, N. Ekins-Daukes, R. A. Taylor, and C. N. Markides, "A review of solar hybrid photovoltaic-thermal (PV-T) collectors and systems," *Progress in Energy and Combustion Science*, vol. 97, p. 101072, 2023/07/01/ 2023. doi: 10.1016/j.pecs.2023.101072

[40] P. J. Pritchard and J. W. Mitchell, *Fox and McDonald's Introduction to Fluid Mechanics*: Wiley, 2016. Available: https://books.google.com/books?id=2gFhBgAAQBAJ.

[41] T. L. Bergman, *Fundamentals of Heat and Mass Transfer*: Wiley, 2011.

[42] R. L. Finney, M. D. Weir, and F. R. Giordano, *Thomas' calculus: early transcendentals*: Addison-Wesley, 2001.

[43] C. S. Solanki, *Solar Photovoltaics: Fundamentals, Technologies And Applications*: PHI Learning, 2015.

[44] K. E. Amori and H. M. T. Al-Najjar, "Analysis of thermal and electrical performance of a hybrid (PV/T) air based solar collector for Iraq," *Applied Energy*, vol. 98, pp. 384-395, 2012. doi: 10.1016/j.apenergy.2012.03.061

[45] M. Alktranee, Q. Al-Yasiri, M. A. Shehab, P. Bencs, Z. Németh, and K. Hernadi, "Experimental and numerical study of a photovoltaic/thermal system cooled by metal oxide nanofluids," *Alexandria Engineering Journal*, vol. 94, pp. 55-67, 2024. doi: 10.1016/j.aej.2024.03.050.

[46] M. Sardarabadi and M. Passandideh-Fard, "Experimental and numerical study of metal-oxides/water nanofluids as coolant in photovoltaic thermal systems (PVT)," *Solar Energy Materials and Solar Cells*, vol. 157, pp. 533-542, 2016. doi: 10.1016/j.solmat.2016.07.008.

[47] J. K. Hale, "Functional differential equations," in *Analytic Theory of Differential Equations: The Proceedings of the Conference at Western Michigan University, Kalamazoo, from 30 April to 2 May 1970*, 2006, pp. 9-22.

[48] F. Esmailie, H. Ghadamian, and M. Aminy, "Transport phenomena study in a solar spouted bed dryer within a draft tube," *Environmental Progress & Sustainable Energy*, vol. 37, pp. 488-497, 2018. doi:10.1002/ep.12670.